

Inventory of Supplemental Information

SUPPLEMENTAL DATA

- Figure S1, related to Figure 1
- Figure S2, related to Figures 2 and 3
- Figure S3, related to Figure 5
- Figure S4, related to Figure 6
- Figure S5, related to Figure 6
- Table S1, Related to Figure 4

SUPPLEMENTAL EXPERIMENTAL PROCEDURES

SUPPLEMENTAL REFERENCES

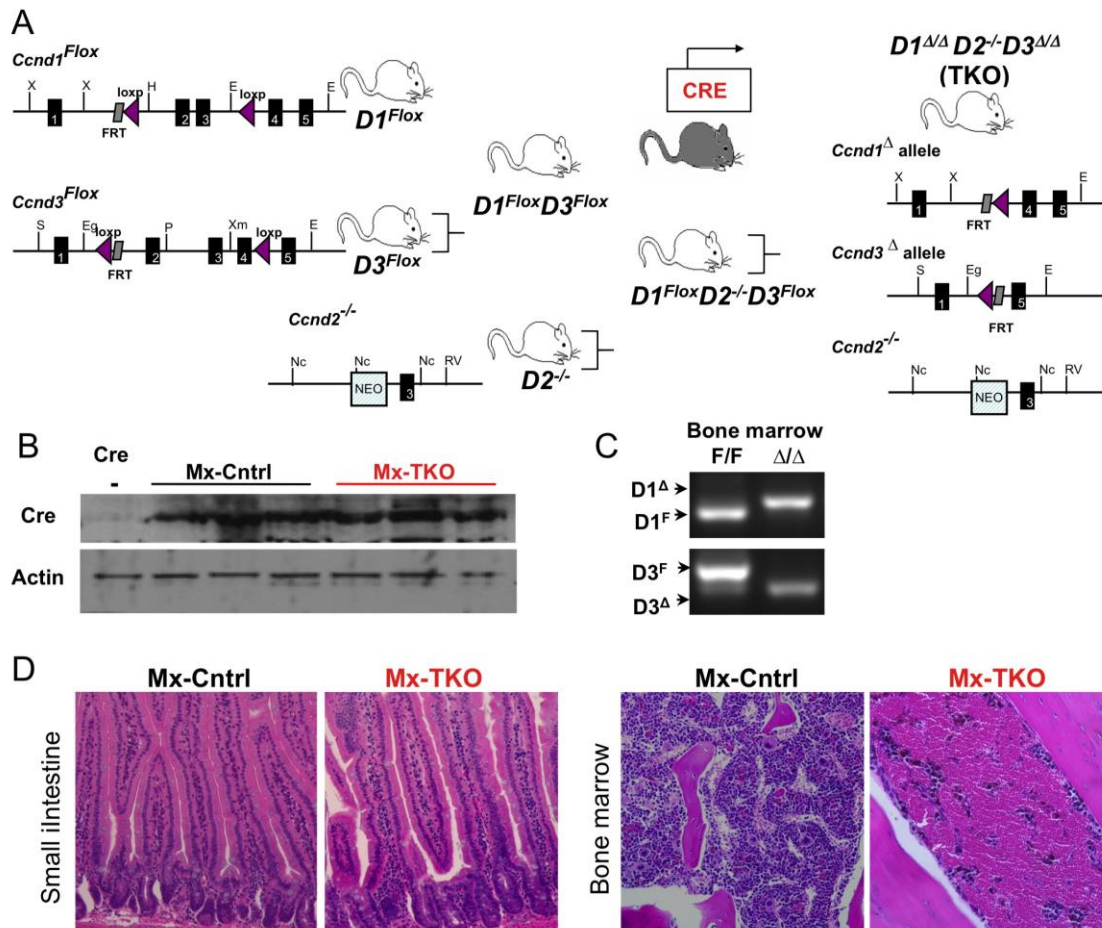


Figure S1. Generation and Analyses of Conditional Cyclin D Triple Knockout Mice, Related to Figure 1

(A) Schematic diagram of breeding to generate cyclin $D1^{F/F}D2^{-/-}D3^{F/F}$ mice.

(B) Western blot analysis of Cre expression levels. Mx-Cre⁺; $D1^{F/F}D2^{-/-}D3^{F/F}$ (MxTKO) and control Mx-Cre⁺; $D1^{F/+}D2^{+/-}D3^{F/+}$ (MxCntrl) animals were treated with pl-pC as described in the Experimental Procedures, and the levels of Cre recombinase in the bone marrow were determined by western blotting. Each lane corresponds to a separate animal of the indicated genotype. As a negative control, bone marrow from a Cre-negative animal was analyzed. (Cre -).

(C) Quantification of deletion efficiency of cyclin $D1^{F/F}$ and cyclin $D3^{F/F}$ loci in Mx1-Cre; $D1^{F/F}D2^{-/-}D3^{F/F}$ animals following pl-pC treatment. Genomic DNA was isolated from bone marrow cells of untreated (F/F) and treated (Δ/Δ) mice and analyzed by semi-quantitative PCR.

(D) Histological appearance of bone marrow and small intestine (a control organ in which MxCre is not expressed) in Mx-Cre⁺; $D1^{F/+}D2^{+/-}D3^{F/+}$ (MxCntrl) and in Mx-Cre⁺; $D1^{F/F}D2^{-/-}D3^{F/F}$ (MxTKO) animals. Mice were treated with pl-pC as described in the Experimental Procedures. Apart from the loss of bone marrow cells in MxTKO mice, no abnormalities were detected in other organs of MxTKO or MxCntrl mice (for example, in the intestine presented in this Figure, as well as in other organs - data not shown).

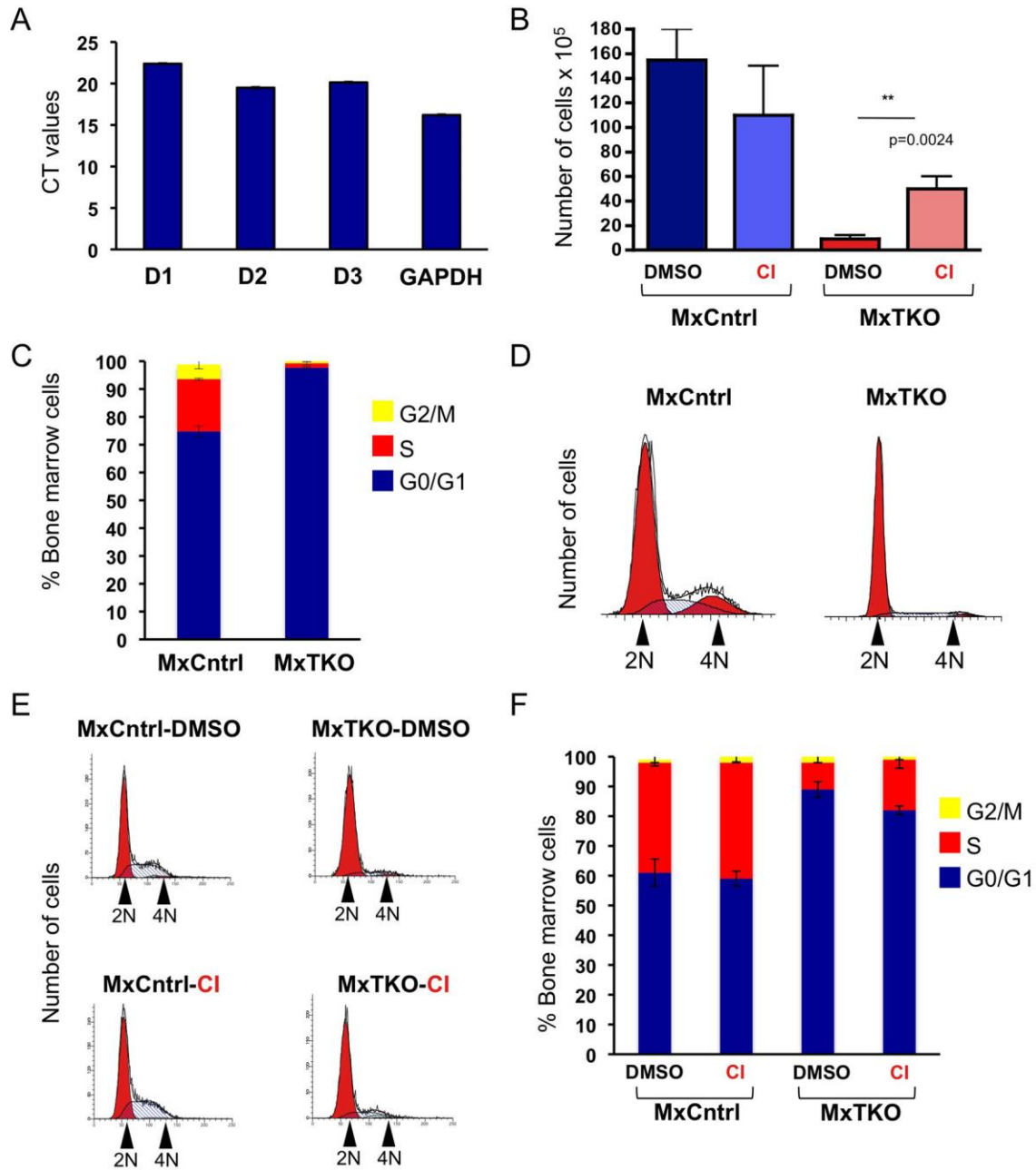


Figure S2. Analyses of Cyclin D Function in Hematopoietic Cells, Related to Figures 2 and 3

(A) The levels of cyclin D1, D2 and D3 transcripts in hematopoietic stem cells from wild-type mice were determined by RT-qPCR. Shown are mean CT values. Error bars, SD.

(B) MxTKO and MxCntrl mice were injected with a caspase inhibitor (CI) or with vehicle only (DMSO) concomitantly with pi-pC injection (to delete D-cyclins in MxTKO mice). The total numbers of bone marrow cells were determined for n=5

animals per group, six days after treatment. Shown are mean values \pm SD. Note that CI treatment increased by 5.5 fold the number of cells remaining after cyclin D ablation (please compare: MxTKO/DMSO versus MxTKO/CI). The rescue is not complete because ablation of D-cyclins caused not only bone marrow cell apoptosis, but also cell cycle arrest (please see below, panels C and D). Treatment with a caspase inhibitor blocked apoptosis, but it had no major impact on cell cycle arrest (please see below, panels E and F).

(C and D) Cell cycle arrest of hematopoietic cells following ablation of D-cyclins. Total bone marrow cells were stained for BrdU incorporation and with propidium iodide and were analyzed by FACS, 4 days after pl-pC injection. (C) Shown are mean percentages \pm SD of cells in the indicated cell cycle phases. (D) Propidium iodide staining of total bone marrow cells analyzed by FACS and plotted using Modfit software.

(E and F) MxTKO and MxCntrl mice were injected with caspase inhibitor (CI) or with vehicle only (DMSO) concomitantly with pl-pC injection (to delete D-cyclins in MxTKO mice), as in (B). (E) Cell cycle analysis of “rescued” cells (gated on TUNEL-negative). Cells were subsequently stained with propidium iodide for DNA content and analyzed by FACS using Modfit software. (F) Mean percentages of TUNEL-negative bone marrow cells in the indicated phase of cell cycle, analyzed as in (E). n=5 per group. Error bars indicate SD.

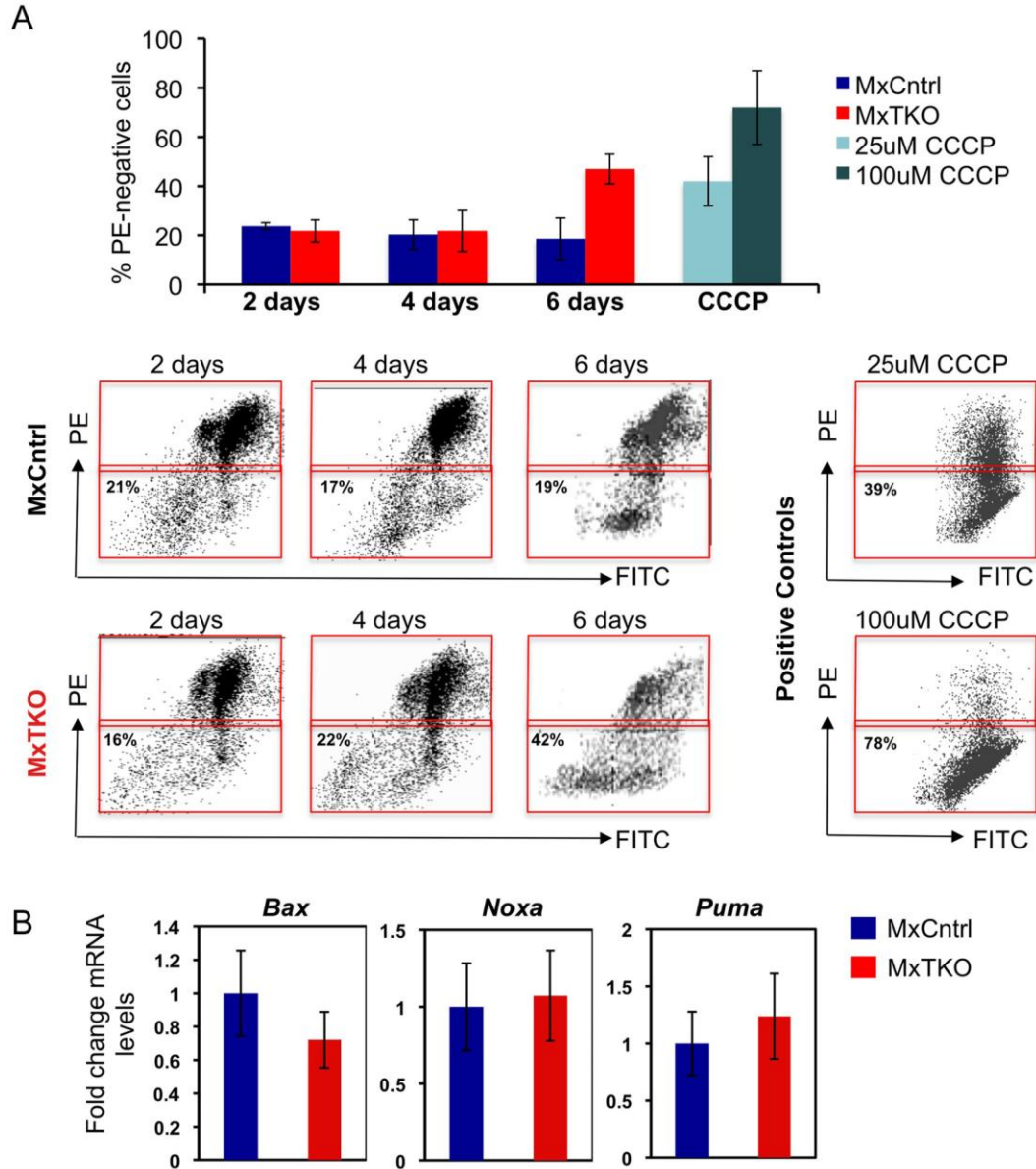


Figure S3. Molecular Analyses of Apoptotic Cells, Related to Figure 5

(A) Analyses of mitochondrial membrane potential following ablation of D-cyclins. MxCntrl and MxTKO mice were injected with 1-3 doses of pl-pC (to delete D-cyclins in MxTKO mice). Bone marrow cells were collected at the indicated time-points, stained with Mitoprobe™ JC-1 Assay Kit (Life Technologies), and analyzed by FACS. As a positive control, MxCntrl bone marrow cells were treated with 25 or 100 μ M carbonyl cyanide 3-chlorophenylhydrazone (CCPP) for 10 min and analyzed in parallel. Upper panel shows mean percentage of PE-negative cells. Error bars denote SD. Representative FACS scatterplots are shown in the lower panel.

(B) The relative levels of Bax, Noxa and Puma transcripts in bone marrow cells of MxCntrl and MxTKO mice were determined by RT-qPCR. Bone marrows were

collected 2 days after pl-pC administration. Shown are mean values, error bars denote SD.

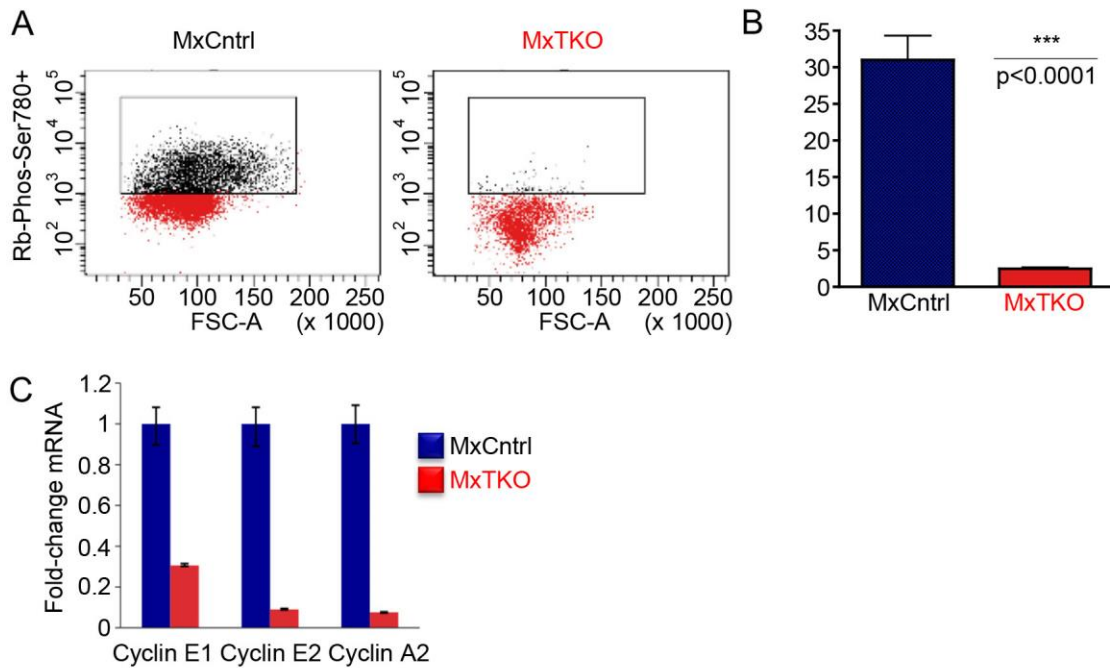


Figure S4. Analyses of Bone Marrow Cells, Related to Figure 6

(A) Reduced phosphorylation of the retinoblastoma protein on a cyclin D-CDK-specific Ser780 residue (Rb-Phos-Ser780+) following ablation of D-cyclins. MxCntrl and MxTKO mice were injected with 2 doses of pl-pC (to delete D-cyclins in MxTKO mice). Bone marrow cells were collected 2 days following the last dose, cells were fixed and permeabilized, stained for phosphorylated Rb-Ser780 and analyzed by FACS. FSC, forward scatter.

(B) Mean percentage of Rb-Phos-Ser780-positive cells, analyzed as in (A). Error bars indicate SD. n=3 per group.

(C) Reduced mRNA levels of E2F transcriptional targets in MxTKO mice. Mice were treated with pl-pC as in (A). The levels of the indicated transcripts were determined by reverse transcription followed by quantitative PCR (RT-qPCR).

Shown are mean values, \pm SD.

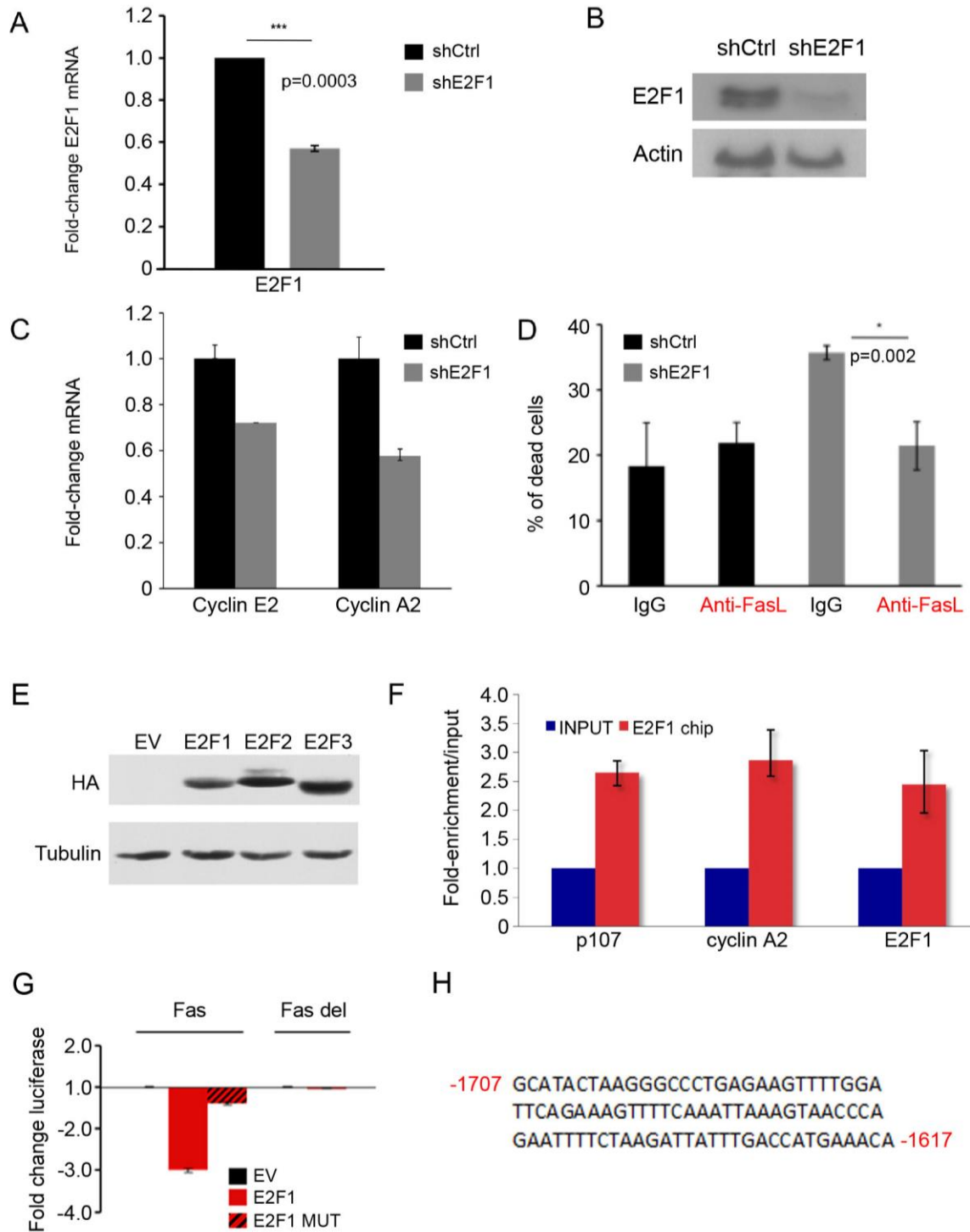


Figure S5. Analyses of the Role of E2F1 in Apoptosis Triggered by Ablation of D-cyclins, Related to Figure 6

(A) Total bone marrow cells were transduced with a lentivirus expressing anti-E2F1 shRNA (shE2F1) or a non-targeting hairpin sequence, (shCtrl). The levels of E2F1 transcripts were analyzed by RT-qPCR. Please note that bone marrow

cells did not undergo any selection after viral transduction. Therefore, E2F1 knockdown took place only in a fraction of cells.

(B) Bone marrow cells were co-transduced with lentiviruses expressing anti-E2F1 shRNA (or a non-targeting hairpin sequence, shCtrl) and GFP. Cells were then sorted for GFP expression, and GFP-positive cells were analyzed by immunoblotting.

(C) Bone marrow cells were transduced with lentivirus expressing anti-E2F1 shRNA, and did not undergo selection (as in A). Transcript levels of two E2F targets, cyclin A2 and cyclin E2, for which E2F was shown to play an activating role, were determined by reverse transcription followed by quantitative PCR (RT-qPCR). As expected, their levels were reduced upon knockdown of E2F1. Data represent mean \pm SD of three replicates.

(D) Bone marrow cells were transduced with lentiviruses encoding anti-E2F1 shRNA (shE2F1), or with control shRNA (shCtrl), and did not undergo selection (as in A). Cells were cultured in the presence of neutralizing anti-FasL antibody (clone MFL3) or IgG (control). Shown are mean percentages of trypan blue positive (dead) cells. Note that anti-FasL antibody inhibited the apoptosis triggered by knockdown of E2F1. See also Figures 6D-6G in the main text.

(E) Analysis of protein levels of ectopically expressed HA-tagged E2Fs, using an anti-HA antibody, from the experiment shown in the main text in Figure 6H.

(F) Chromatin immunoprecipitation (ChIP) analysis of E2F1 binding to promoter regions of three known E2F1 targets in HSPC. Anti-E2F1 antibody from Santa Cruz was used (antibody #1 in Figure 6I). Data represent mean \pm SD of three replicates.

(G) Promoter-luciferase constructs driven by the wild-type Fas promoter (Fas), or Fas promoter with the deleted 90 bp E2F1-binding region (Fas del) were co-transfected with vectors encoding E2F1, or E2F1 DNA binding/transactivation-deficient mutant (E2F1 MUT), or with an empty vector (EV). Please also see Figure 6H in the main text.

(H) DNA sequence of the 90 bp "E2F1-responsive element" in the human Fas promoter. No classical E2F-binding sites (TTTSSCGC) were found in this segment. However, Cao et al. (2011) observed, using anti-E2F1 ChIP-seq, that the great majority of genomic E2F1-binding sites do not contain this motif.